Full Paper

Journal of the Brazilian Chemical Society

https://dx.doi.org/10.21577/0103-5053.20260075

J. Braz. Chem. Soc. **2026**, *37*, e-20260075, 1-15

Effect of Biomass Types on the Slow and Fast Pyrolysis Products Through Elemental and Physicochemical Evaluation

Lisiane O. Diehl,[a] *Dian Celante,*[a] *Samuel R. Waechter,*[b] *Fábio A. Duarte,*[b] *Fernanda de Castilhos*[a] *and Paola A. Mello*[*,b]

[a]*Departamento de Engenharia Química, Universidade Federal de Santa Maria (UFSM), 97105-900 Santa Maria-RS, Brazil*

[b]*Departamento de Química, Universidade Federal de Santa Maria (UFSM), 97105-900 Santa Maria-RS, Brazil*

In the present study, pine wood and sugarcane straw were chosen to represent the biomass classes of forest and agricultural residues. Lignocellulosic biomasses were submitted to slow and fast pyrolysis in an experimental-scale laboratory unit at temperatures ranging from 400 to 600 °C. The solid (biochar) and liquid (bio-oil) products were characterized, and physicochemical properties and chemical composition were analyzed. Experimental results revealed significant differences depending on the biomass type and the pyrolysis conditions. An increasing in heating rate and pyrolysis temperature led to higher liquid phase yields and enhanced higher heating values of the solid phase. Proximate analysis of biochar showed notable variations in moisture, ash, volatile matter and fixed carbon contents, while infrared spectroscopy indicated differences in functional groups. Bio-oil analyses showed similar water content and acid values across the investigated conditions, indicating limited sensitivity to process parameters, although significant differences were observed among biomass types. Elemental analyses covered metals, as alkaline and alkaline earth elements, as well as Cl, P and S. Results demonstrated that some elements remained in higher concentrations in biochar, being Al, Ca and, K the predominant inorganic constituents. In contrast, bio-oil presented lower concentration of elements, with Al and S as the major contaminants.

Keywords: lignocellulosic biomass, biochar; bio-oil, composition, pine wood, sugarcane straw

Introduction

Lignocellulosic biomass constitutes an abundant and renewable feedstock with considerable potential to supply the constant increase in energy demand.[1] This type of biomass does not compete with food crops, is considered a carbon-neutral material, and can be the source to produce biofuels or to be converted into value-added chemicals through different conversion mechanisms.[2] Biofuels represent a promising alternative to reduce dependence on fossil fuels and minimize the emission of atmospheric pollutants. There are several techniques for converting lignocellulosic biomass into biofuels, and one of the most studied is thermochemical conversion through pyrolysis processes.[3]

Pyrolysis is based on endothermic reactions that decomposes the biomass at temperatures typically ranging from 300 to 700 °C in the absence of oxygen. This process leads to the thermochemical conversion of biomass into three-phase products: solid (biochar), liquid (bio-oil), and gaseous (biogas). The amount and properties of each product depend on the type of raw material and the operating conditions because it can be carried out in different temperature ranges, heating rates, and residence steam times.[4,5] Pyrolysis has received considerable attention due to its simplicity and speed. Also, the process might yield versatile products, which are quite easy to handle and collect, unlike other types of thermochemical biomass conversion processes.[6,7] Pyrolysis is classified into many types (e.g., slow, fast, flash, microwave-assisted, catalytic) according to the difference in operating conditions. Furthermore, the type of reactor and its configuration can facilitate the yield of a given product.[5,8]

Among the types of pyrolysis, slow and fast processes generate different major products. Slow pyrolysis involves a broad range of temperatures (from 300 to 800 °C), which are increased gradually with a slow heating rate and with

*e-mail: paola.mello@ufsm.br
Editor handled this article: Izaura C. N. Diógenes (Executive)

a longer vapor residence time (10 to 60 min), appropriate for forming stable carbonaceous solid biochar materials.[9] Fast pyrolysis is considered thermal decomposition route at a medium temperature range (from 400 to 600 °C) with a higher heating rate, shorter vapor residence time (0.5 to 10 s), high heat transfer rate and fast speed cooling of pyrolysis vapor. These conditions are advantageous for higher bio-oil yield. Fast pyrolysis has been studied as a promising thermochemical conversion route for the production of sustainable biofuels and a wide range of value-added, and commercially relevant chemicals.[5,10] Some authors have reported that changing experimental and operational conditions, as well as the type of reactor, influenced the yield, physicochemical properties, and elemental composition of the products from pyrolysis of pine wood (PW)[11,12] and sugarcane straw (SS).[13,14] For example, for PW pyrolysis, by using a stainless-steel reactor at temperatures from 400 to 900 °C, it was reported that the biochar yield decreased with increasing pyrolysis temperature. This behavior is attributed to the enhanced volatilization of biomass components.[15] In addition, it was observed that increasing the pyrolysis temperature significantly influenced the physicochemical properties of the resulting products, especially the concentration of elements, promoting carbon enrichment and reducing the relative content of hydrogen and oxygen, as a result of intensified devolatilization and oxygen-removal reactions.[16] For SS pyrolysis, a study using a pilot plant with a fluidized bed reactor, comparing the temperatures of 600 and 900 °C, with a heating rate of 5 °C min^{-1}, showed that the increasing temperature resulted in more gaseous products and less liquid and solid fraction.[13] On the other hand, at a higher heating rate (15 °C min^{-1}) and 600 °C, more liquid and gas amount was obtained.[13] Using the same raw material, these studies demonstrated the influences of different process conditions.

Pine forests are important source of raw material for the wood industry, generating substantial amounts of residues during harvesting and industrial processing, including branches, bark, and sawdust, which are often improperly disposed of.[8] Sugarcane straw, generated during sugarcane harvest, has increased in recent years due to the expansion of mechanized harvesting and high crop productivity, resulting in large amounts of straw partially left on the field for soil protection.[17] In this context, SS and PW are typical examples of agricultural and forestry by-products that are abundant and underutilized. The importance of these residues is evidenced by the large number of works involving the study of different applications with these lignocellulosic biomasses for producing biofuels and energy.

Considering the increasing demand for clean and renewable energy sources, the present study aimed to process PW and SS biomasses through experimental-scale laboratory pyrolysis system at slow and fast conditions, to compare the yield under different experimental conditions and investigate some characteristics of the main products. A fixed-bed reactor system based on recent studies[18-22] was used, and the influence of the biomass type on the elemental composition of the biomass and pyrolysis products was the main feature evaluated. Although the pyrolysis of lignocellulosic biomasses has been previously investigated, systematic and integrated comparisons under equivalent experimental conditions remain limited. Most previous studies have focused on individual feedstocks or specific process parameters, rather than providing a comprehensive evaluation that includes detailed characterization of both biomasses and their resulting pyrolysis products.[23,24] The present paper aims to contribute for understanding the correlation of composition and thermochemical conversion of woody and non-woody biomasses and biochar and bio-oil production. This approach provides fundamental insights into the suitability of bio-oil as a precursor for fuel upgrading and highlights the potential of biochar as a value-added carbon material for environmental, agricultural, and industrial applications.

Experimental

PW was collected as forest residue from Brazilian forests and SS was collected as agricultural residue from Brazilian sugarcane harvest fields. These biomasses were submitted to pyrolysis at different operating parameters and produced biochar and bio-oil were characterized, as described in the following sections.

Biomass preparation

PW and SS were quartered into small pieces. Then, the biomasses were passed through a 2 mm sieve and dried in an oven (ETC 45 model, Nova Ética, Brazil) with air circulation at 105 °C for 2 h. For pyrolysis, the samples were used after drying. For raw materials characterization, the samples were crushed again into smaller particles (< 840 μm) using a knife mill (TE 048 model, Marconi, Brazil).

Biomass characterization

Proximate analysis was conducted following the ASTM E871 standard[25] for the moisture content, ASTM E872[26] for the volatile matter, and ASTM D1102[27] for the ash content, using a muffle furnace (0913 model,

Jung, Brazil). Fixed carbon content was estimated by difference. The biomass composition analysis was performed following the TAPPI T203[28] and TAPPI T222[29] for cellulose, hemicellulose and lignin content. For extractives content, the TAPPI T204[30] standard was used for pine wood biomass and the ASTM D1105 standard[31] for sugarcane straw biomass. Elemental analysis of metals, Cl, S, and P, was conducted following the ISO 16967:2015 (Method A) standard,[32] using a microwave-assisted single reaction chamber (SRC-UltraWAVE™ system, Milestone, Italy) for wet digestion. The concentration of metals, Cl, S, and P was determined in the digests by inductively coupled plasma optical emission spectrometry (ICP OES, Spectro Ciros, CCD Spectro Analytical Instruments, Germany) using the conditions described in Supplementary Information (SI) section, Table S1. The N concentration was determined using an elemental analyzer (Multi EA 5000 Elemental Analyzer, Analytik Jena, Germany) according to ASTM D5762[33] for total nitrogen (TN).

Experimental apparatus and procedure

An experimental laboratory-scale fixed-bed pyrolysis system was designed, assembled, and commissioned, and subsequently operated for the first time in this study. A schematic representation of the experimental setup is shown in Figure 1. The reactor consisted of stainless-steel tubular vessel (with 25 cm length and 33.5 mm diameter), which was placed inside an electric furnace (2.8 kW, special model, Sanchis, Brazil) to provide controlled heating during pyrolysis experiments. On the top of the reactor, a special joint was used for positioning the inlet of the nitrogen and a type K thermocouple, which was positioned in the middle of the reactor and connected to a proportional-integral-derivative (PID) temperature controller. At the bottom of the reactor, a stainless-steel filter (40 μm pore size, Porofil, Brazil) was fixed to hold the sample and separate the solid phase from the liquid and gas phases. The reactor outlet was directly attached to a copper coil condenser, which was immersed in an ice bath (0 °C) to condense the vapors to collect the liquid phase. The non-condensable gas phase was passed through a scrubber before exhaustion. About 25 g of PW and 8 g of SS pre-dried were separately placed in the reactor for each experiment. The reactor was closed until locked and inserted into the electric furnace. The gas valve was opened to purge, and the controller was turned on according to the setpoint temperature. The biomasses were pyrolyzed and evaluated at temperatures of 400, 500, and 600 °C at 10 and 100 °C min^{-1} of heating rate. Upon reaching the desired temperature, the pyrolysis time was set to 15 min to ensure complete pyrolysis. Finally, the bio-oil was collected, and after cooling the reactor, the biochar was also collected. For all experiments, high-purity nitrogen (> 99.9999%, White Martins) was used at 0.1 and 0.3 L min^{-1} flow-rates to prevent biomass oxidation along the pyrolysis process. Nitrogen was passed through the pyrolyzed biomass after experiments until the samples cooled down to room temperature. A photograph of the system is provided in the SI section (Figure S1).

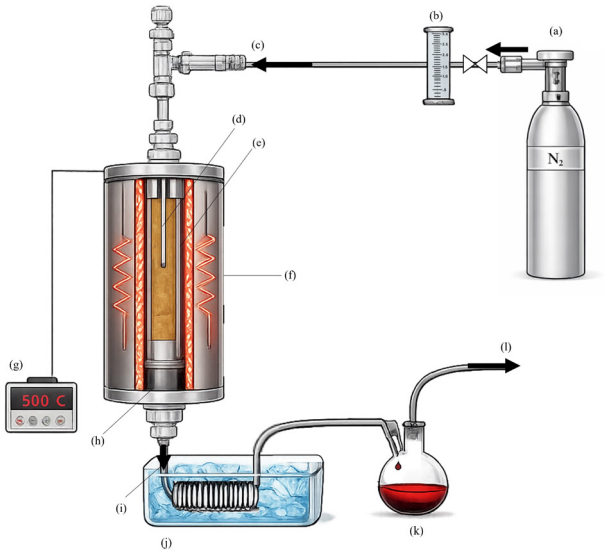

Figure 1. A schematic representation of the fixed bed pyrolysis system. (a) Nitrogen cylinder, (b) flowmeter, (c) gas inlet, (d) thermocouple, (e) stainless steel reactor, (f) electric tube furnace, (g) controller, (h) stainless steel filter, (i) copper condenser coil, (j) water bath, (k) condensed liquid phase, (l) gas outlet.

In the end, the yield of the products was calculated using equations 1 and 2, where $W_{biomass}$ is the initial weight of biomass and $W_{biochar}$ and $W_{bio\text{-}oil}$ are the resulting weight of each product after pyrolysis. The biogas yield was calculated by difference.

$$Yield_{biochar}\,(\%) = W_{biochar} / W_{biomass,dry\ basis} \times 100 \quad (1)$$

$$Yield_{bio-oil}\,(\%) = W_{bio-oil} / W_{biomass,dry\ basis} \times 100 \quad (2)$$

Analytical methods for characterizing the pyrolysis products

After pyrolysis experiments, the liquid and solid products were collected and prepared for different types of analysis based on common parameters reported on the literature and supported by the analytical framework described previously.[34] For the biochars, proximate analysis was conducted following the standard procedures reported in ASTM D3173[35] for moisture, ASTM D3174[36] for ash, and ASTM D3175[37] for the volatile matter. Fixed carbon content was estimated by difference. Nitrogen and chlorine contents

were determined using an elemental analyzer (Multi EA 5000 Elemental Analyzer, Analytik Jena, Germany) according to ASTM D5762[33] for total nitrogen (TN) and ASTM D5808[38] for total chlorine (TCl). Functional groups were analyzed by Fourier transform infrared spectroscopy (FTIR, IRPrestige-21, Shimadzu, Japan) in the wavenumber range from 400 to 4000 cm^{-1}. The infrared spectrum was collected with KBr pellets. The higher heating value (HHV) was measured by calorimetry (model 6400 EAI Automatic Isoperibol Calorimeter, Paar Instrument Company, USA). A laser diffraction particle size analyzer (Mastersizer 2000, Malvern, United Kingdom) was used to analyze the particle size distribution of the biochar before grinding. Metals, S and P in biochar were determined following the ISO 16967:2015 (Method A) standard[33] by ICP OES after wet digestion. Additional details regarding sample preparation and ICP OES determination are described in the SI section (Table S1).

For the bio-oils, the water content was determined in an automatic titrator (Titrando 836, Metrohm, Switzerland) with platinum double wire electrode (6.0338.100 model, Metrohm, Switzerland) following the ASTM E203 standard.[39] The acid value was measured using the same automatic titrator with lithium chloride electrode and combined glass membrane for a non-aqueous medium (6.0229.100, Metrohm, Switzerland) following the ASTM D664.[40] Metals, S and P content in bio-oil was determined by ICP OES after sample preparation by adapting a method previously developed.[41] Further details are described in the SI section (Tables S1, S7, S8 and S9).

Statistical analysis

Data were analyzed using Statistica 12 software (TIBCO Software Inc., California, USA, 2014). Initially, one-way analysis of variance (ANOVA) followed by Tukey's honestly significant difference (HSD) as a *post hoc* test was used, with 95% of confidence level in all cases to verify statistically significant differences between mean values. Tukey's indices, when applied, were expressed by different letters indicating significant differences between groups.

In addition, to evaluate the influence of temperature, biomass type and heating hate, a complete experimental design was used in triplicate, generating 36 runs. Temperature was evaluated in three levels (400, 500, and 600 °C) while biomass type (PW and SS) and heating rate (10 and 100 °C min^{-1}) in two levels. The responses of the experimental design were biochar and bio-oil yields. A three-factor factorial ANOVA was performed for the assessment of main interaction effects among variables. Effect estimates, regression coefficients, and significance levels were obtained from the fitted factorial model using pure error as the residual term. Statistical significance was considered at $p < 0.05$. This combined statistical approach enabled both comparison of mean values and evaluation of the individual and combined influence of process variables on pyrolysis product distribution.

Results and Discussion

Biomass analysis

Lignocellulosic composition analysis

The lignocellulosic composition of biomasses used in this study is presented in Table 1. The composition of PW is consistent with values typically reported for softwood species, which contain 40-50 wt.% cellulose, 19-35 wt.% hemicellulose and 21-30 wt.% lignin on a dry basis.[42] Sugarcane straw composition was in agreement with previous studies reporting that sugarcane-derived biomass contains mainly cellulose and hemicellulose, about 65-70 wt.% in dry mass[42,43] while lignin component is present in smaller amounts (about 20-25 wt.% of the dry mass).[44,45] Some characteristics of these biomasses, such as physicochemical and elemental analysis performed in this study, can be directly associated with the relative proportions of these structural components, which strongly influence the thermal decomposition behavior and conversion during pyrolysis.[42]

Proximate analysis

Table 2 lists the results of proximate analysis for PW and SS biomasses. The analysis for moisture was made as received, and for others, the PW and SS were ground and dried. High moisture content means that extra heat can be necessary, and the thermal conversion efficiency of

Table 1. Composition analysis for PW and SS biomasses (n = 3)

Sample	Cellulose / (wt.%, dry basis)	Hemicellulose / (wt.%, dry basis)	Lignin / (wt.%, dry basis)	Extractives / (wt.%, dry basis)
PW	41.0 ± 0.5	24.5 ± 1.8	26.3 ± 1.2	3.86 ± 0.11
SS	29.7 ± 0.1	37.7 ± 0.3	21.0 ± 0.08	7.40 ± 0.14

PW: pine wood; SS: sugarcane straw.

Table 2. Proximate analysis of PW and SS biomasses (n = 3)

Sample	Moisture / (wt.%)	Ash / (wt.%, dry basis)	Volatile matter / (wt.%, dry basis)	Fixed carbon / (wt.%, dry basis)
PW	9.50 ± 0.08	2.38 ± 0.02	75.87 ± 1.08	21.74 ± 1.09
SS	6.83 ± 0.29	3.63 ± 0.03	80.77 ± 0.92	15.60 ± 0.62

PW: pine wood; SS: sugarcane straw.

biomass can be reduced. Biomass moisture values were within the expected content since moisture content should be less than 10% for the pyrolysis process.[45] With regard to the ash content, which demonstrates an approximation of the bulk inorganic matter, results were low for both PW and SS. Volatile matter represents the content that can burn in an inert atmosphere, which is CO_2, CO, and H_2 gases, light molecular weight compounds, and moisture present in the composition of biomasses and, in heating at 950 °C for 10 min, the tars that are driven off as gas.[46] Results were similar to those in previous reports for PW and SS,[47] as well as the low fixed carbon content. The reasonably high volatile matter content in both biomasses suggests a promising capacity to produce bio-oil or biogas.[46,47] Proximate analysis showed statistically significant differences between both types of biomasses.

Elemental analysis

Table 3 shows the main inorganic composition of biomasses. The major elements of the PW and SS biomasses were Al, Ca and K. Similar results were reported in previous studies for PW[48] and SS.[14] The elemental content of both biomasses reflects mainly the concentrations of metal ions in the soil, water, metals from stones, and dirt particles, from which the tree can take up the metal ions at the root membranes. Also, there are multiple ways to contaminate biomasses with chemical elements, such as using materials, contamination from equipment used for harvesting, sampling, and transportation, among others.[5] The remaining composition is related to the concentration of the elements in the biomass[44] and should be determined as they can impact the thermochemical conversion.[49]

Concerning the biomass type, the concentration of most elements was considerably higher in SS than in PW biomass, except for Ba, Mn and Zn. This inorganic content is expected to significantly influence pyrolysis process as elements can act as catalysts during thermal degradation. They were related to promote primary and secondary reactions such as cracking, dehydration, and decarboxylation, thereby modifying the decomposition pathways of lignocellulosic components and the distribution of pyrolysis products.[50] The formation of solid and gaseous products can be affected and the yield of condensable organic vapors can be reduced due to enhanced cracking of intermediate compounds.[25] Furthermore, inorganic elements can also affect the chemical composition, stability and quality of the bio-oil, influencing its physicochemical properties and potential applications.[25,50,51]

Table 3. Elemental composition of PW and SS biomasses (n = 3)

Analyte	PW biomass / (μg g^{-1})	SS biomass / (μg g^{-1})
Al	1006 ± 25	2149 ± 75
Ba	13.5 ± 0.1	14.4 ± 0.9
Ca	1569 ± 58	2852 ± 109
Cl	104 ± 2	503 ± 3
Cu	< 6.0[b]	< 6.0[b]
Fe	837 ± 104	1693 ± 69
K	1007 ± 6	3670 ± 45
Mg	403 ± 5	1179 ± 42
Mn	139 ± 3	44.1 ± 1.6
N[a]	3382 ± 13	5669 ± 42
Na	< 337[b]	< 371[b]
P	125 ± 10	325 ± 8
S	196 ± 14	639 ± 11
Sr	12.7 ± 0.4	17.3 ± 0.9
Ti	135 ± 10	328 ± 16
Zn	11.5 ± 0.2	10.5 ± 0.7

[a]Elemental analyser; [b]LOQ: limit of quantification. PW: pine wood; SS: sugarcane straw.

Analysis of the effects of the pyrolysis variables

Main and interaction effects

Results of biochar and oil yield according to the experimental design are presented in Table S2 (SI section). Factorial ANOVA data are shown in SI (Tables S3 and S4, SI section). The results demonstrated that pyrolysis temperature was the most significant factor affecting both biochar and bio-oil yields ($p < 0.001$).

The negative effect of temperature on biochar yield (effect = −15.94) may be associated to enhanced devolatilization and secondary cracking at higher temperatures, reducing solid residue formation. Conversely,

the strong positive effect on bio-oil yield (effect = +15.11) suggests increased formation of condensable volatiles due to intensified depolymerization of cellulose, hemicellulose and lignin at elevated thermal severity. These trends are consistent with established pyrolysis mechanisms reported in the literature.[52,53]

Heating rate also significantly influenced product distribution. Fast pyrolysis resulted in lower biochar yield (effect = −5.14) and higher bio-oil yield (effect = +5.29), which can be attributed to rapid heat transfer and shorter vapor residence times, which limits secondary cracking reactions.[23,52]

Regarding biomass type, its effect on biochar yield was not statistically significant ($p = 0.191$), but it significantly influenced bio-oil yield (effect = −2.36; $p < 0.001$). Differences in lignin content and inorganic composition are known to modify thermal degradation pathways and catalytic cracking reactions during pyrolysis.[24,54]

Furthermore, the significant three-factor interaction (temperature × heating rate × biomass) observed for both biochar and bio-oil yields ($p < 0.01$) confirm that product distribution results from the combined and interdependent influence of all process variables. This finding highlights the importance of integrated analysis approaches, as pyrolysis behavior cannot be fully explained by evaluating parameters independently. Similar interaction effects have been reported in recent studies, demonstrating that temperature, heating rate, and biomass composition jointly determine reaction kinetics, vapor evolution, and final product yields.[24,52,53]

Effect of pyrolysis temperature on product yields for SS and PW biomass

According to Tables S3 and S4, pyrolysis temperature was the most significant factor for bio-oil and biochar yield. In slow pyrolysis, thermal degradation begins with moisture removal and initial bond cleavage, followed by the progressive decomposition of biomass constituents such as hemicellulose, cellulose, lipids and proteins. These primary reactions generate volatiles and intermediate compounds, while prolonged residence times favor secondary reactions and the formation of carbon-rich residues (biochar). In contrast, fast pyrolysis employs high heating rates and short vapor residence times, minimizing secondary cracking and repolymerization reactions, thereby enhancing the yield of condensable vapors and promoting bio-oil production.[55] As lignocellulosic biomasses are mainly composed of hemicellulose, lignin, and cellulose, the yield and the elemental and physicochemical properties of the pyrolysis products are directly linked to these main compounds, which leads to differences in thermal decomposition. In the present work, the thermal decomposition of PW and SS biomasses was processed in the 400 to 600 ºC range with 10 ºC min^{-1} as heating rate for slow pyrolysis (S) and 100 ºC min^{-1} for fast pyrolysis (F). The results for each biomass are presented and discussed below, separately for PW and SS. For more details and statistical analysis for yield of the products, by comparing both biomasses, results in SI section (Table S5) demonstrated significant differences related to biomass type and pyrolysis condition for biochar and bio-oil products. For non-condensable gases, very little or no difference was identified.

Yield from pine wood pyrolysis

In slow pyrolysis, the lowest temperature showed a higher yield for the solid phase when compared to other processes, according to Tukey's test. By evaluating at 400 and 600 °C (with 10 ºC min^{-1}), the largest amount of PW biochar (48.2%) was obtained at 400 °C. Results also showed that lower temperatures, regardless of the rate, enhanced the amount of solid produced. In contrast, in fast pyrolysis the maximal bio-oil content was obtained under high reaction temperature (600 °C), producing 54.7% of the liquid phase. This behavior is associated with increased volatilization at higher temperatures, favoring the formation of condensable organic vapors.[51] The lowest bio-oil yields were obtained at the lowest temperature, indifferently of the heating rate. Some authors reported yield results for pyrolysis of this biomass, but the differences in experimental conditions proved crucial to reach out similar values.[11,56] The results are shown in Figure 2 and are compared with yield from SS pyrolysis (Table 4) for statistical analysis through Tukey's test (as will be discussed). The assays were performed in triplicates for each experimental condition, and the results are presented in SI section (Table S5).

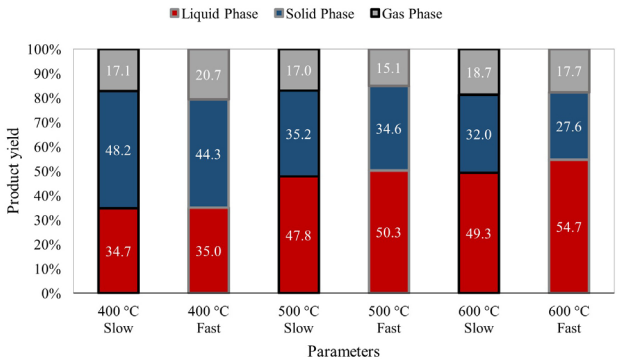

Figure 2. Yield of the products from slow and fast pyrolysis of PW biomass in the temperature range of 400-600 °C (n = 3).

Yield from sugarcane straw pyrolysis

Similar behavior for SS biomass was observed, as can be seen in Figure 3. However, for this feedstock, the heating rate had a more pronounced influence on product yields at 400 and 500 °C. When comparing experiments conducted at the same temperature but under different heating rate (slow or fast pyrolysis), the differences in yield were more significant than those observed for PW for analogous conditions. For example, slow pyrolysis at 500 °C led to a higher biochar yield than fast pyrolysis performed at the same temperature. For biochar, the highest yield was 48.5%, obtained at 400 °C through slow pyrolysis. The optimal condition to produce bio-oil from SS biomass was also achieved at 600 °C as fast pyrolysis conditions (100 ºC min^{-1}), resulting in 52.8% of the liquid phase. These findings have important implications for biofuel production, as higher liquid yields at elevated temperatures enhance biomass-to-liquid conversion efficiency and increase the availability of feedstock for subsequent upgrading processes, such as catalytic hydrotreatment.[10] Comparing these two biomasses,

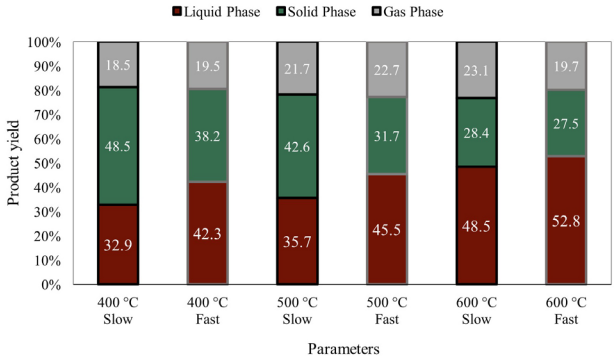

Figure 3. Yield of the products from slow and fast pyrolysis of SS biomass in the temperature range of 400-600 °C (n = 3).

SS produced a greater amount of non-condensable gases than PW biomass in all process conditions, except for fast pyrolysis at 400 °C, similar to that was observed in previous reports.[44,45] However, this difference is not considerable in several experimental conditions, as proved by Tukey's test, as seen in Table 4. Similarity in the biochar yield obtained at 400 °C from both biomasses was also seen. Other experimental conditions presented differences according to the biomass type in this product yield. For bio-oil yield, the significant differences are associated with the change of parameters. Differences related to the amount of products, reactor design, and also biomass preparation were reported in previous studies.[49,57] All the results for the pyrolysis of SS biomass are presented in the SI section (Table S5).

Biochar analysis

The images of PW and SS biochar produced in the present study are presented in the SI section (Figure S2). By increasing the temperature, the biochars showed smaller particle sizes. The biochar derived from PW and SS were nominated as "PW xxxY", where "xxx" is the pyrolysis temperature and "Y" is the type of process (S to slow and F to fast). It was also possible to notice the elimination of the brown color, indicating alterations in the original molecular structure of the biomasses.

Proximate analysis

Table 5 lists the results of proximate analysis for PW and SS biochars. The results showed that all biochars mainly comprise of fixed carbon and volatile matter. For PW and SS biochars, the moisture content ranged from 2.93 to 5.54%, and there were no significant differences between the biomasses and process parameters. The ash

Table 4. Yield of the products for pyrolysis of PW and SS biomass through slow and fast pyrolysis (n = 3)

Biomass	Pyrolysis parameters	Biochar yield / wt.%	Bio-oil yield / wt.%	Biogas yield / wt.%
PW	400 °C slow	48.2 ± 0.8^{d}	34.7 ± 0.7^{c}	17.1 ± 1.4^{ac}
PW	500 °C slow	35.2 ± 0.5^{bc}	47.8 ± 1.1^{ab}	17.0 ± 1.2^{ac}
PW	600 °C slow	32.0 ± 0.8^{ab}	49.3 ± 0.3^{ab}	18.7 ± 1.1^{abcd}
PW	400 °C fast	44.3 ± 1.4^{d}	35.0 ± 2.1^{c}	20.7 ± 1.2^{abde}
PW	500 °C fast	34.6 ± 2.2^{bc}	50.3 ± 1.5^{abd}	15.1 ± 1.5^{c}
PW	600 °C fast	27.6 ± 0.8^{a}	54.7 ± 1.3^{d}	17.7 ± 0.6^{abc}
SS	400 °C slow	48.5 ± 1.7^{d}	32.9 ± 0.9^{c}	18.5 ± 1.0^{abc}
SS	500 °C slow	42.6 ± 4.2^{ef}	35.7 ± 3.6^{c}	21.7 ± 2.2^{bde}
SS	600 °C slow	28.4 ± 0.8^{a}	48.5 ± 0.8^{ab}	23.1 ± 1.3^{e}
SS	400 °C fast	38.2 ± 1.6^{ce}	42.3 ± 1.6^{e}	19.5 ± 0.6^{abde}
SS	500 °C fast	31.7 ± 2.9^{ab}	45.8 ± 3.1^{ae}	22.7 ± 2.3^{de}
SS	600 °C fast	27.5 ± 0.8^{a}	52.8 ± 1.5^{bd}	19.7 ± 1.8^{abde}

Different letters mean significant difference for the same yield by Tukey's test. PW: pine wood; SS: sugarcane straw.

content of PW biochar was very low in both types of pyrolysis (maximum 4.75%) and increased with increasing temperature and vapor residence time. For SS biochar, ash content (minimum 5.78%, maximum 12.10%) was notably higher than PW biochar. In addition, SS biochar demonstrated that by increasing vapor residence time, the ash content decreased; contrarily, the ash content increased with increasing temperature. Moreover, the considerable quantity of fixed carbon content expressed to be favorable for the recovery of biochar through pyrolysis[58] and reveals the development of adsorption sites because the carbon structure, which would be the fixed carbon, is then developed into pores.[59] The significant amount of volatile matter content in PW and SS biochars produced under low-temperature conditions (400 °C) implies the potential of these substances to be converted into liquid and gaseous products (e.g., biogas and biofuel) for application as a potential fuel or chemical feedstock for pyrolysis process.[58] The same trend for volatile matter and fixed carbon in PW biochar was reported by other authors,[12,60] and the differences in the moisture and ash content were also reported in previous studies.[34] For SS biochar, it was also observed that increasing pyrolysis temperature resulted in higher fractions of fixed carbon due to an increased release of volatile matter.[49] Regarding the biomass type, volatile matter and fixed carbon did not show relevant differences. There was a notable difference only in relation to the pyrolysis parameters for these two properties.

High heating value (HHV)

The HHV is presented in Figure 4 for the raw biomass and produced biochar from slow pyrolysis at 400 and 600 °C and from fast pyrolysis at 600 °C. This evaluation is suitable for evaluating the combustibility of the materials since they have the potential for application as solid fuels. Beyond that, this analysis is suitable for comparing biochar with non-processed biomass since its value is usually low to use in certain applications.[60] HHV analysis was performed for PW and SS biochar pyrolyzed at 400 and 600 °C through slow pyrolysis, and the biochar from both biomasses pyrolyzed at 600 °C through fast pyrolysis. These samples were selected to verify if there were significant changes when increasing temperature and heating rate. In addition to these samples, *in natura* biomasses of PW and SS were also evaluated to perform a comparative study between processed and non-processed materials. It was observed that the HHVs decreased with the increase in heating rate and decreasing pyrolysis temperature. The pyrolysis temperature proved to have more influence on HHV when compared to the heating rate. It was verified by statistical evaluation (Tukey's test) that the HHV for *in natura* biomass was lower than those for biochar, showing a difference of about 10 MJ kg^{-1}. Also, HHV significantly increased with increasing temperature. According to the literature,[12] high temperatures can cause some bonds rupture and high-energy chemical bonds formation occurs, increasing the HHV of biochar products. Other differences in HHVs refer to the type of biomass (forest and agricultural biomass) and the ash content, which absorb the amount of energy released during combustion.[60] Processed and non-processed PW biomass revealed statistically significant differences, and higher values were observed than processed and non-processed SS biomass. Similar HHV for SS, PW, and different types of lignocellulosic biomass was observed previously,[46,61] and increased HHV with pyrolysis temperature for biochar was also reported.[47,61] Typically, biochar had a high calorific value compared to biomasses due to their lower proportion of H and O than C.[46]

Table 5. Proximate analysis for PW and SS biochar for different pyrolysis parameters (n = 3)

Sample	Moisture / wt.%	Ash / wt.%	Volatile matter / (wt.%, dry basis)	Fixed carbon / (wt.%, dry basis)
PW 400S	3.39 ± 0.30^{ab}	3.38 ± 0.18^{a}	74.0 ± 1.7^{e}	22.6 ± 1.5^{bc}
PW 500S	5.54 ± 0.43^{c}	3.54 ± 0.1^{a}	39.4 ± 0.7^{a}	57.0 ± 0.6^{a}
PW 600S	5.45 ± 0.11^{bc}	4.75 ± 0.40^{e}	30.1 ± 0.2^{d}	65.1 ± 0.7^{f}
PW 400F	3.63 ± 0.34^{abc}	0.81 ± 0.16^{b}	58.2 ± 0.30^{b}	40.1 ± 0.3^{e}
PW 500F	4.14 ± 0.16^{abc}	1.50 ± 0.06^{b}	45.0 ± 1.7^{a}	53.5 ± 1.8^{a}
PW 600F	4.18 ± 0.42^{abc}	3.00 ± 0.27^{a}	42.0 ± 0.44^{a}	55.1 ± 0.8^{a}
SS 400S	4.07 ± 0.41^{abc}	5.72 ± 0.30^{c}	63.4 ± 2.0^{bc}	30.8 ± 1.7^{d}
SS 500S	4.07 ± 0.33^{abc}	8.90 ± 0.11^{d}	69.9 ± 1.8^{ce}	21.2 ± 2.0^{b}
SS 600S	3.76 ± 0.22^{abc}	12.10 ± 0.10^{g}	30.9 ± 4.0^{d}	56.9 ± 3.9^{a}
SS 400F	2.93 ± 0.76^{a}	5.95 ± 0.28^{c}	64.1 ± 2.8^{bc}	30.0 ± 2.4^{cd}
SS 500F	4.73 ± 2.07^{abc}	9.30 ± 0.05^{d}	62.4 ± 1.1^{bc}	28.3 ± 1.0^{bcd}
SS 600F	3.37 ± 0.67^{ab}	10.06 ± 0.82^{f}	39.5 ± 2.1^{a}	50.5 ± 2.9^{a}

Different letters mean significant difference for the same property by Tukey's test. PW: pine wood; SS: sugarcane straw; S: slow; F: fast.

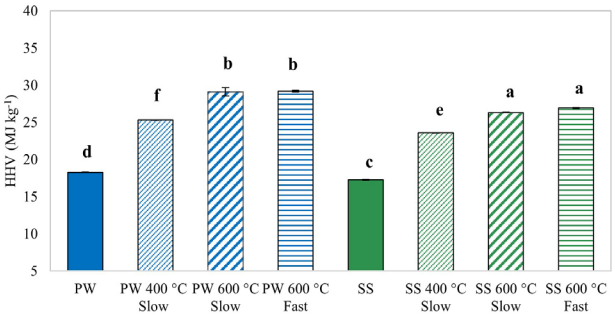

Figure 4. HHV for PW and SS biomasses and PW and SS biochar. Different letters indicate significant differences by Tukey's test (n = 2).

Elemental analysis

The diverse elemental composition in biochar can be related to the multi-functionality of this material, with distinctive functional features and structures.[62] Understanding the inorganic composition of biochar is vital for many reasons, which depend on applications. The overabundance of some elements may result in toxicity. Analysis of feedstock inorganic content (biomass) compared with biochar inorganic content can give insight into losses of inorganic elements during pyrolysis or contamination from processing, storage, or pyrolysis equipment.[34] This study analyzed all the biochar samples through an elemental analyzer to determine if N and Cl concentration change with increasing temperature and heating rate. Beyond that, the biochar from PW and SS pyrolyzed at 600 °C and 100 °C min^{-1} were digested and analyzed by ICP OES to determine the concentration of metals and P and S.

Table 6 reveals N and Cl concentrations in PW and SS biochar. For PW biochar, increasing the temperature and heating rate decreases the amount of N. For Cl, in general, the opposite occurs. The highest concentration of Cl was determined at 600 °C and fast pyrolysis conditions. Although SS biochar presented a very similar behavior, the amount of N and Cl was higher than that of PW biomass biochar. Thus, from the applied statistical test, the effect of the biomass type was remarkable.

Table 7 shows the concentration of metals and P and S in PW and SS biochar at 600 °C and 100 °C min^{-1}. Some studies demonstrated that biochar derived from herbaceous biomass expressed higher content of these elements than that derived from woody biomass.[44] Also, the process temperature can influence the final composition of inorganic elements, increasing or decreasing the concentration of these elements by changing experimental conditions.[63] It is essential to observe that the elemental concentration in the biochars was substantially higher than the concentration of elements in the biomass. Higher content of Al, Ca, K, Mg, and S was determined in SS biochar. This significant amount of Ca and K may be due to the feedstocks, typically rich in alkaline elements from the soil.[64] Heavy metals, such as Fe, was higher in SS biochar than PW biochar, which agrees with the biomass composition before pyrolysis. The type of raw material used for biochar production is a key factor, as the concentration of elements varies significantly. For the Mn element, PW biochar demonstrated a higher concentration than SS biochar, differently for all other elements.

Table 6. Elemental analysis of N and Cl for PW and SS biochar pyrolyzed at 400 to 600 °C through slow and fast pyrolysis (n = 3)

Sample	N / (μg g^{-1})	Cl / (μg g^{-1})
PW 400S	2010 ± 20^{c}	50.4 ± 4.8^{a}
PW 500S	1090 ± 12^{e}	112 ± 0.5^{b}
PW 600S	836 ± 51^{d}	153 ± 0.5^{b}
PW 400F	1880 ± 42^{b}	36.0 ± 1.0^{a}
PW 500F	1725 ± 22^{g}	38.0 ± 3.0^{a}
PW 600F	1489 ± 2^{f}	148 ± 3^{b}
SS 400S	2439 ± 14^{a}	358 ± 9^{c}
SS 500S	2487 ± 11^{a}	292 ± 7^{e}
SS 600S	1883 ± 28^{b}	425 ± 13^{d}
SS 400F	2638 ± 50^{h}	374 ± 17^{cd}
SS 500F	2508 ± 21^{a}	561 ± 3.3^{f}
SS 600F	2123 ± 32^{c}	712 ± 44^{g}

Different letters mean significant difference for the same element by Tukey's test. PW: pine wood; SS: sugarcane straw; S: slow; F: fast.

Table 7. Elemental analysis for PW and SS biochar by ICP OES (n = 3)

Analyte	PW biochar / (μg g^{-1})	SS biochar / (μg g^{-1})
Al	2263 ± 100	5164 ± 129
Ba	37.5 ± 0.6	188 ± 5
Ca	4053 ± 162	10917 ± 205
Cu	< 16^{a}	< 16^{a}
Fe	1484 ± 62	3425 ± 70
K	2385 ± 33	11971 ± 188
Mg	1146 ± 32	4461 ± 131
Mn	417 ± 8	146 ± 5
Na	< 1211^{a}	< 1211^{a}
P	361 ± 6	1223 ± 16
S	< 454^{a}	1017 ± 20
Sr	34.9 ± 0.6	64.3 ± 1.6
Ti	196 ± 6	596 ± 32
Zn	44.8 ± 8.1	218 ± 65

^{a}LOQ: limit of quantification. PW: pine wood; SS: sugarcane straw; S: slow; F: fast.

Functional groups analysis by FTIR

As shown in Figures 5 and 6, experimental data obtained from FTIR spectra in PW and SS biochar are

presented. The main FTIR spectrum bands identified in biochar are summarized in the SI section (Table S6). The functional groups obtained from the FTIR spectra demonstrate the carbohydrate structures of cellulose, hemicellulose, and lignin through oxygenated hydrocarbon bonds[65] in both raw materials. For both PW and SS biochar, it was possible to verify that the loss of intensity in bands due to stretching of O–H and aliphatic C–H bonds and the increase in the intensity of bands due to the aromatic C–H bonds suggests that dehydration and aromatization reactions occurred.[66] It was impossible to notice significant changes in biochar from slow pyrolysis, which means that the decrease in heating rate does not change the organic structure.

Particle size distribution

Particle size distribution and cumulative particle size of PW and SS from fast and slow pyrolysis at 600 °C was measured (SI section, Figure S3). Cumulative diameter (d (0.1), d (0.5), d (0.9)) and mean diameter were used to calculate the PDI (polydispersity index) (Table 8). The parameters d (0.1), d (0.5) and d (0.9) represent the particle diameters below which 10, 50, and 90% of the sample volume are found, respectively. Samples with the same temperature and different heating rates were chosen to verify if this parameter can change the particle diameter size. It was possible to observe that the increase in the heating rate for PW biochar did not cause significant differences. In contrast, SS biochar demonstrated changes in particle size distribution as the heating rate increased. Also, the Sauter mean diameter practically has reduced by half with increasing heating rate for this biochar.

Among the selected biochar, SS 600F revealed the lowest mean diameter, d (0.1), d (0.5) and d (0.9). It is possible to consider that extensive devolatilization and decomposition at about 600 °C occur and bond formation is the main reaction at 600 °C. This restructuring process provides a structurally ordered biochar that would not break easily during grinding. Therefore, a higher number of larger particles would be available, as shown in particle size analysis data (Table 8).[22] It was also visible that the PW biochar demonstrated the highest PDI, indicating that this

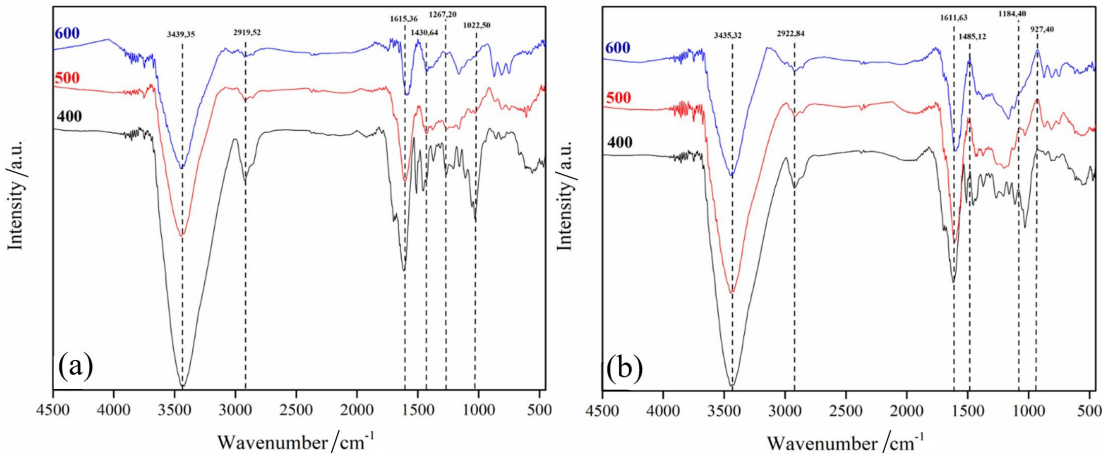

Figure 5. FTIR (KBr) spectra of PW biochar from (a) fast and (b) slow pyrolysis at 400 to 600 °C.

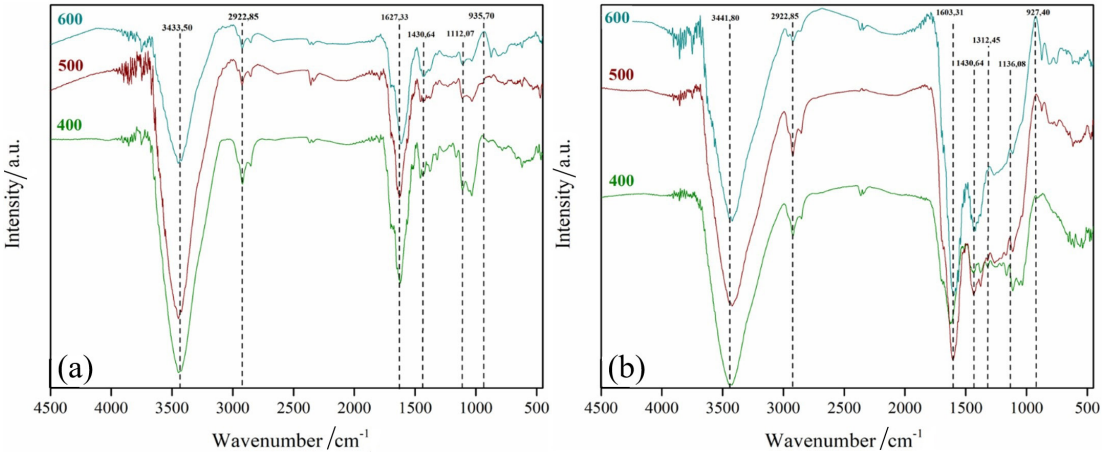

Figure 6. FTIR (KBr) spectra of SS biochar from (a) fast and (b) slow and pyrolysis at 400 to 600 °C.

Table 8. Biochar particle size distribution and PDI

Sample	Sauter mean diameter / μm	Distribution percentiles			PDI
	(d_{32})	d (0.1)	d (0.5)	d (0.9)	
PW 600S	218.31	106.90	512.74	1254.10	2.15
PW 600F	209.32	103.80	492.00	1159.37	3.20
SS 600S	181.77	87.74	784.50	1475.49	2.24
SS 600F	93.90	43.20	226.51	768.49	1.77

PDI: polydispersity index; PW: pine wood; SS: sugarcane straw; S: slow; F: fast.

type of raw material pyrolyzed at 600 °C and 100 °C min^{-1} is a heterogeneous sample.

Bio-oil analysis

Water content

The liquid yield reached for PW and SS biomasses was about 50%. A significant part of this percentage is an aqueous phase, and another part is an oil phase. The water content in the PW bio-oils separated both phases due to the high water content of bio-oil and high molecular weight polar compounds.[67] The phase separation was not visibly identified in the SS bio-oils, perhaps due to the low amount of liquid product and the polarity of major compounds. The pyrolysis condensation process is responsible for most of the water content since fractions of bio-oils collected at different temperatures demonstrated variable amounts of water.[13] Also, when using a high moisture feedstock (> 10 wt.%), a two-phase product with a larger aqueous and viscous oily phase may be produced. Ageing reactions were also related to the formation of two phases and water separation is usually reported when its content in bio-oil exceeded 30 wt.%.[68] In the same study, some metals, mainly K, were related to more water production due to the catalysis of reactions.[68] Beyond that, operational and experimental conditions, system design, type of reactor, product separation setup, and sampling are other factors that can influence the water content of bio-oils.[69] Due to the phase separation, there is a significant loss of organic matter from the target bio-oil (oil phase) to the aqueous phase[70] and this could be considered a challenge to this process.[68]

Water content was measured for all bio-oil samples produced through slow and fast pyrolysis, and the results are shown in Figure 7a. The phase at the bottom (non-aqueous) for PW bio-oils was analyzed, resulting in a significant variation from 3.71 to 33.3%. The samples were shaken before measurement for SS bio-oils, resulting in a variation from 25.2 to 33.4% in fast pyrolysis, as

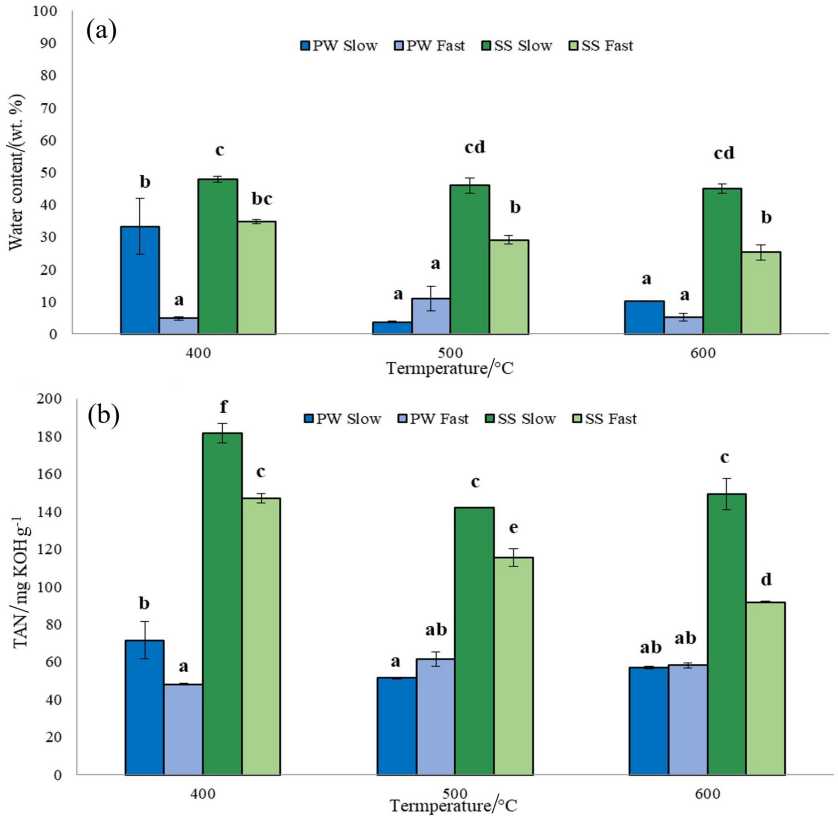

Figure 7. Water content (a) and (b) total acid number of pyrolyzed PW and SS bio-oils at 400-600 °C and 10-100 °C min^{-1}. Different letters indicate significant differences by Tukey's test.

reported previously[71] and 44.9 to 47.9% in slow pyrolysis. SS bio-oils showed to be influenced by heating rate, since by decreasing the heating rate, the water content increased, as well as PW bio-oil pyrolyzed at 400 °C. Contrarily, no significant differences when increasing temperature was observed for SS bio-oil. The larger amount of water content was measured in bio-oils pyrolyzed at 400 °C for both biomasses. However, the SS bio-oils demonstrated the highest amount for all parameters of the pyrolysis process when compared to the PW bio-oils, as verified by Tukey's test. Previous studies[69] demonstrated that liquid products from agricultural residues are nonhomogeneous, having high (39-51 wt.%) water content. The water content of liquid products correlates with physical properties such as density, viscosity, and heating value, which are very important characteristics to apply bio-oils as biofuels.

Acidity

The amount of potassium hydroxide (KOH, mg) that reacts to neutralize the acids in 1 g of bio-oil can be related to the corrosivity of the bio-oil, represented by the concentration of acid constituents.[72] To be used as biofuel, bio-oils must have low levels of acidity. High acidity can lead to degradation and affect cold biofuel properties such as filter clogging and freezing points.[73] This method provided statistically comparable results in terms of the type of biomass and process conditions (Figure 7b). SS bio-oils presented the highest acid values. Considering the process parameters for PW bio-oils, the results showed no significant change with increasing temperature and heating rate. However, some trends to lower acidity for higher temperatures can be observed for bio-oils from SS.[61] The results indicated the highest acidity indexes at 400 °C through slow pyrolysis, using both PW and SS for pyrolysis. It could be assumed that a high content of sterically hindered acidic groups would cause difficulties for the hydrodeoxygenation of bio-oils pyrolyzed at 400 °C. On the other hand, these macrostructures might be broken down at higher temperatures into monocyclic phenolic compounds that can easily be further hydrodeoxygenated.[70] Increasing the heating rate for PW bio-oils reduced the total acid number for the pyrolyzed bio-oil at 400 °C. At 500 and 600 °C, changing the process parameters, there was no significant variation in the acidity indexes. The high standard deviation of the measurements was also notable, indicating the heterogeneity of this type of sample. Similar results for PW bio-oils were reported[72] by comparing different standards and shelf times of bio-oils. In contrast, SS bio-oils presented high acidity indexes, mainly for the lowest temperature and heating rate. The total acid number (TAN) of the SS bio-oil samples ranged from 91.8 to 182 mg KOH g^{-1}. Bio-oil from fast pyrolysis at 600 °C represented the lowest index, indicating that, a high temperature is necessary for the SS biomass to remove the acids present in this sample. Lower TAN was reported previously for bio-oils from SS,[13] using the same standard for measurement.

Elemental analysis

Some elements, such as alkali metals, can increase the propensity for degradation of bio-oils and can cause engine corrosion. Generally, the elemental analysis of bio-oil obtained in this work revealed a relatively low content of metals, P and S. Table 9 shows the elemental composition of PW and SS bio-oils pyrolyzed at 600 °C and 100 °C min^{-1}. The major element for bio-oils from both biomasses was S, but bio-oil from agricultural biomass (SS) proved to contain the largest amount, as observed for the raw biomass. The concentration of S in bio-oils must be controlled when applied as a biofuel due to the possibility of producing SO_x. For all elements, PW bio-oils showed the lowest elemental concentrations.[67] Other elements were present in very low concentrations when related to the amount in the raw biomass. This may have occurred due to the filter placed in the system to separate the phases of the products in the pyrolysis reactor. Similar values for S, Na, and K for the PW bio-oil were reported in previous studies.[69]

Table 9. Elemental analysis for PW and SS bio-oils by ICP OES (n = 3)

Analyte	PW bio-oil / (μg g^{-1})	SS bio-oil / (μg g^{-1})
Al	14.4 ± 1.5	20.6 ± 3.5
Ba	0.08 ± 0.01	0.17 ± 0.02
Ca	< 0.7[a]	2.73 ± 0.06
Cu	3.23 ± 0.50	23.9 ± 4.1
Fe	< 0.7[a]	7.00 ± 1.26
K	< 19[a]	< 19[a]
Mg	< 1.0[a]	1.22 ± 0.14
Mn	< 0.02[a]	< 0.02[a]
Na	2.05 ± 0.30	9.40 ± 2.84
P	2.40 ± 0.47	4.76 ± 0.90
S	42.7 ± 1.7	155 ± 10
Sr	< 0.07[a]	0.112 ± 0.002
Ti	< 0.2[a]	< 0.2[a]
Zn	< 0.8[a]	< 0.8[a]

[a]LOQ: limit of quantification. PW: pine wood; SS: sugarcane straw.

Conclusions

Two different biomass types (pine wood and sugarcane straw) were converted into bio-oils, biochar and biogas through slow and fast pyrolysis in an experimental laboratory-scale fixed-bed reactor. Physicochemical and

elemental characterization of the biomasses and pyrolysis products demonstrated that both biomass type and process parameters significantly influenced product distribution and properties. Factorial ANOVA indicated that pyrolysis temperature was the main factor affecting biochar and bio-oil yields, with higher temperatures reducing biochar formation and increasing bio-oil production due to enhanced devolatilization.

Biochar properties changed with increasing temperature, showing higher moisture, ash, and fixed carbon contents, while the concentration of N and Cl decreased from 400 to 600 °C. Infrared spectra indicated the predominance of functional groups associated with oxygenated hydrocarbons derived from carbohydrate structures of cellulose, hemicellulose, and lignin. Differences in particle size distribution were observed between PW and SS biochars under similar grinding conditions, although both materials showed improved grindability after pyrolysis.

Most bio-oil samples presented water content below 30 wt.% and acid values comparable to those reported in the literature, although additional pretreatment may be required for direct applications. Regarding inorganic elements, Al, Ca and K were the most abundant in biochar, whereas Al and S was the major element in bio-oil. These characteristics indicate that the pyrolysis liquids obtained have potential for further use, particularly after upgrading processes aimed at improving stability and reducing oxygenated compounds. Furthermore, the elemental analysis enabled evaluating the mass balance between the raw materials and the pyrolysis products. Overall, the results demonstrate that biomass type and pyrolysis conditions significantly influence the physicochemical properties of biochar and bio-oil. These findings provide valuable information for optimizing thermochemical processes and contribute to the development of biomass-derived fuels and products as sustainable alternatives within the renewable industry and biofuel sectors.

Supplementary Information

Supplementary data are available free of charge at http://jbcs.sbq.org.br as PDF file.

Data Availability Statement

All data supporting the findings of this study are available within the article and its supplementary information.

Acknowledgments

The authors are grateful to Programa de Recursos Humanos da Agência Nacional do Petróleo, Gás Natural e Biocombustíveis (PRH-ANP - process number 23081.047655/2019-11), FINEP, CNPq (process 314254/2023-4 for P. A. Mello, process 305870/2019-0 for F. Castilhos), FAPERGS (process 0167-7) and CAPES (Financial Code 001) for supporting this study. The Figure 1 and Graphical Abstract were prepared with the assistance of ChatGPT (OpenAI, GPT-5.3 version), which was used for image refinement, layout optimization, and visual suggestions. All final content was reviewed and validated by the authors.

Author Contributions

All the authors contributed to the study's conception and design. L. O. D.: conceptualization, data curation, formal analysis, investigation, methodology, validation, writing original draft. D. C.: data curation, investigation, methodology. S. R. W.: formal analysis, methodology, validation. F. A. D.: methodology, writing (review and editing). F. C.: methodology, conceptualization, funding acquisition, writing (review and editing). P. A. M.: conceptualization, data curation, funding acquisition, methodology, project administration, resources, supervision, writing (review and editing).

References

1. Güleç, F.; Parthiban, A.; Umenweke, G. C.; Musa, U.; Williams, O.; Mortezaei, Y.; Suk-Oh, H.; Lester, E.; Ogbaga, C. C.; Gunes, B.; Okolie, J. A.; *Biofuels, Bioprod. Biorefin.* **2024**, *18*, 755. [Crossref]
2. Putro, J. N.; Soetaredjo, F. E.; Lin, S.-Y.; Ju, Y.-H.; Ismadji, S.; *RSC Adv.* **2016**, *6*, 46834. [Crossref]
3. Brindhadevi, K.; Anto, S.; Rene, E. R.; Sekar, M.; Mathimani, T.; Thuy Lan Chi, N.; Pugazhendhi, A.; *Fuel* **2021**, *285*, 119106. [Crossref]
4. Canabarro, N.; Soares, J. F.; Anchieta, C. G.; Kelling, C. S.; Mazutti, M. A.; *Sustainable Chem. Processes* **2013**, *1*, 22. [Crossref]
5. Sekar, M.; Mathimani, T.; Alagumalai, A.; Chi, N. T. L.; Duc, P. A.; Bhatia, S. K.; Brindhadevi, K.; Pugazhendhi, A.; *Fuel* **2021**, *283*, 119190. [Crossref]
6. Lee, S. H.; Eom, M. S.; Yoo, K. S.; Kim, N. C.; Jeon, J. K.; Park, Y. K.; Song, B. H.; Lee, S. H.; *J. Anal. Appl. Pyrolysis* **2008**, *83*, 110. [Crossref]
7. Eom, M. S.; Lee, S. H.; Yoo, K. S.; Park, Y. K.; Lee, J. G.; Kim, J. H.; *Energy Sources, Part A:* **2013**, *35*, 1225. [Crossref]
8. Goyal, H. B.; Seal, D.; Saxena, R. C.; *Renewable Sustainable Energy Rev.* **2008**, *12*, 504. [Crossref]
9. Hodgson, E.; Lewys-James, A.; Rao Ravella, S.; Thomas-Jones, S.; Perkins, W.; Gallagher, J.; *Bioresour. Technol.* **2016**, *214*, 574. [Crossref]
10. Bridgwater, A. V.; *Biomass Bioenergy* **2012**, *38*, 68. [Crossref]

11. Fraga, L. G.; Teixeira, C.; Ferreira, M. E. C.; Teixeira, S. F.; Vilarinho, C.; Gonçalves, M. M.; *Energies* **2022**, *15*, 5253. [Crossref]
12. Liu, Z.; Han, G.; *Fuel* **2015**, *158*, 159. [Crossref]
13. Durange, J. A. C.; Santos, M. R. L.; Pereira, M. M.; Fernandes Jr., L. A. P.; Souza, M. N.; Mendes, A. N.; Mesa, L. M.; Sánchez, C. G.; Sanchez, E. M. S.; Pérez, J. M. M.; Carvalho, N. M. F.; *J. Biomater. Nanobiotechnol.* **2013**, *4*, 10. [Crossref]
14. de Palma, K. R.; Tomaz, E.; Soria-Verdugo, A.; Silva, M. A.; *Fuel* **2021**, *304*, 121404. [Crossref]
15. Rambhatla, N.; Panicker, T. F.; Mishra, R. K.; Manjeshwar, S. K.; Sharma, A.; *Results Eng.* **2025**, *25*, 103679. [Crossref]
16. Luo, Q.; Deng, Y.; Li, Y.; He, Q.; Wu, H.; Fang, X.; *Sci. Rep.* **2024**, *14*, 25711. [Crossref]
17. Goldoni, E. L.; Sussi, K.; Oliveira, M.; Neto, M. M.; Alan, R.; Ramos, V.; *Res., Soc. Devel.* **2022**, *11*, 1. [Crossref]
18. David, E.; Kopac, J.; *J. Anal. Appl. Pyrolysis* **2018**, *134*, 495. [Crossref]
19. Nagy, G.; Dobó, Z.; *Biomass Bioenergy* **2020**, *139*, 105580. [Crossref]
20. Upadhyay, D. S.; Panchal, K. R.; Sakhiya, A. K. V; Patel, R. N.; *Energy* **2020**, *211*, 118187. [Crossref]
21. Zhu, J.; Jin, L.; Li, J.; Bao, Z.; Li, Y.; Hu, H.; *Bioresour. Technol.* **2019**, *290*, 121739. [Crossref]
22. Farrokh, N. T.; Suopajärvi, H.; Mattila, O.; Sulasalmi, P.; Fabritius, T.; *Fuel* **2020**, *265*, 117017. [Crossref]
23. Vilas-Boas, A. C. M.; Tarelho, L. A. C.; Oliveira, H. S. M.; Silva, F. G. C. S.; Pio, D. T.; Matos, M. A. A.; *Sustainable Energy Fuels* **2023**, *8*, 379. [Crossref]
24. Ding, L.; Cheng, M. H.; Lin, Y.; Lin, K. T.; Sale, K. L.; Sun, N.; Donohoe, B. S.; Ray, A. E.; Li, C.; *Energy* **2025**, *322*, 135697. [Crossref]
25. ASTM E871-82: *Standard Test Method for Moisture Analysis of Particulate Wood Fuels*; ASTM International, West Conshohocken, 2019. [Crossref]
26. ASTM E872-82: *Standard Test Method for Volatile Matter in the Analysis of Particulate Wood Fuels*; ASTM International, West Conshohocken, 2019. [Crossref]
27. ASTM D1102-84: *Standard Test Method for Ash in Wood*; ASTM International, West Conshohocken, 2021. [Crossref]
28. TAPPI T203 cm-22: *Alpha, Beta and Gama-Cellulose in Pulp*; TAPPI Press, 2022. [Crossref]
29. TAPPI T222 om-21: *Acid-Insoluble Lignin in Wood and Pulp, Test Method*; TAPPI Press, 2021. [Crossref]
30. TAPPI T204 cm-17: *Solvent Extractives of Wood and Pulp*; TAPPI Press, 2017. [Crossref]
31. ASTM D1105-21: *Standard Test Method for Preparation of Extractive-Free Wood*; ASTM International, West Conshohocken, 2021. [Crossref]
32. ISO 16967:2015: *Solid Biofuels - Determination of Major Elements. Al, Ca, Fe, Mg, P, K, Si, Na and Ti - Part A*; International Organization for Standardization, 2015. [Crossref]
33. ASTM D5762-24: *Standard Test Method for Nitrogen in Liquid Hydrocarbons, Petroleum and Petroleum Products by Boat-Inlet Chemiluminescence*; ASTM International, West Conshohocken, 2024. [Crossref]
34. Singh, B.; Camps-Arbestain, M.; Lehmann, J.; *Biochar: A Guide to Analytical Method*; National L; CSIRO Publishing: Clayton, Australia, 2017. [Crossref]
35. ASTM D3173-11: *Standard Test Method for Moisture in the Analysis Sample of Coal and Coke*; ASTM International, West Conshohocken, 2017. [Crossref]
36. ASTM D3174-12(2018)E01: *Standard Test Method for Ash in the Analysis Sample of Coal and Coke from Coal*; ASTM International, West Conshohocken, 2020. [Crossref]
37. ASTM D3175-20: *Standard Test Method for Volatile Matter in the Analysis Sample of Coal and Coke*; ASTM International, West Conshohocken, 2020. [Crossref]
38. ASTM D808-23: *Standard Test Method for Determining Chloride in Aromatic Hydrocarbons and Related Chemicals by Microcoulometry*; ASTM International, West Conshohocken, 2023. [Crossref]
39. ASTM E203-16: *Standard Test Method for Water Using Volumetric Karl Fischer Titration*; ASTM International, West Conshohocken, 2023. [Crossref]
40. ASTM D664-18E02: *Standard Test Method for Acid Number of Petroleum Products by Potentiometric Titration*; ASTM International, West Conshohocken, 2024. [Crossref]
41. Druzian, G. T.; Nascimento, M. S.; Picoloto, R. S.; Mesko, M. F.; Flores, E. M. M.; Mello, P. A.; *J. Anal. At. Spectrom.* **2022**, *37*, 1799. [Crossref]
42. Segers, B.; Nimmegeers, P.; Spiller, M.; Tofani, G.; Jasiukaitytė-Grojzdek, E.; Dace, E.; Kikas, T.; Marchetti, J. M.; Rajić, M.; Yildiz, G.; Billen, P.; *RSC Sustainability* **2024**, *2*, 3730. [Crossref]
43. Negrão, D. R.; Grandis, A.; Buckeridge, M. S.; Rocha, G. J. M.; Leal, M. R. L. V.; Driemeier, C.; *Renewable Sustainable Energy Rev.* **2021**, *148*, 111268. [Crossref]
44. Dhyani, V.; Bhaskar, T.; *Renewable Energy* **2018**, *129*, 695. [Crossref]
45. Varma, A. K.; Mondal, P.; *Ind. Crops Prod.* **2017**, *95*, 704. [Crossref]
46. Nanda, S.; Mohanty, P.; Pant, K. K.; Naik, S.; Kozinski, J. A.; Dalai, A. K.; *Bioenergy Res.* **2013**, *6*, 663. [Crossref]
47. Canettieri, E. V.; da Silva, V. P.; Neto, T. G. S.; Hernández-Pérez, A. F.; da Silva, D. D. V.; Dussán, K. J.; das Graças Almeida Felipe, M.; de Carvalho, J. A.; *J. Braz. Soc. Mech. Sci. Eng.* **2018**, *40*, 416. [Crossref]
48. Anca-Couce, A.; Zobel, N.; Berger, A.; Behrendt, F.; *Combust. Flame* **2012**, *159*, 1708. [Crossref]

49. Melo, L. C. A.; Coscione, A. R.; Abreu, C. A.; Puga, A. P.; Camargo, O. A.; *Bioresources* **2013**, *8*, 4992. [Crossref]
50. Giudicianni, P.; Gargiulo, V.; Grottola, C. M.; Alfè, M.; Ferreiro, A. I.; Mendes, M. A. A.; Fagnano, M.; Ragucci, R.; *Energy Fuels* **2021**, *35*, 5407. [Crossref]
51. Chen, W.; Tao, X.; Shi, X.; Guo, W.; Wang, Y.; Liu, B.; Yang, H.; *npj Mater. Sustainability* **2024**, *2*, 25. [Crossref]
52. Jerzak, W.; Acha, E.; Li, B.; *Energies* **2024**, *17*, 5082. [Crossref]
53. Safdari, M. S.; Amini, E.; Weise, D. R.; Fletcher, T. H.; *Fuel* **2019**, *242*, 295. [Crossref]
54. Li, A.; Liu, H.-L.; Wang, H.; Xu, H.-B.; Jin, L.-F.; Liu, J.-L.; Hu, J.-H.; *Bioresources* **2016**, *11*, 3259. [Crossref]
55. Saarela, K.; Harju, L.; Rajander, J.; Lindroos, A.; *Sci. Total Environ*. **2005**, *343*, 231. [Crossref]
56. Wang, Z.; Wang, F.; Cao, J.; Wang, J.; *Fuel Process. Technol.* **2010**, *91*, 942. [Crossref]
57. Charusiri, W.; Vitidsant, T.; *Sustainable Chem. Pharm.* **2017**, *6*, 114. [Crossref]
58. Liew, R. K.; Nam, W. L.; Chong, M. Y.; Phang, X. Y.; Su, M. H.; Yek, P. N. Y.; Ma, N. L.; Cheng, C. K.; Chong, C. T.; Lam, S. S.; *Process Saf. Environ. Prot.* **2018**, *115*, 57. [Crossref]
59. Dhorabe, P. T.; Lataye, D. H.; Ingole, R. S.; *J. Hazard., Toxic Radioact. Waste* **2017**, *21*. [Crossref]
60. Ronsse, F.; Hecke, S. Van; Dickinson, D.; Prins, W.; *GCB Bioenergy* **2013**, *5*, 104. [Crossref]
61. Hassan, E. B. M.; Steele, P. H.; Ingram, L.; *Appl. Biochem. Biotechnol.* **2009**, *154*, 182. [Crossref]
62. Glaser, B.; Wiedner, K.; Seelig, S.; *Agron. Sustainable Dev.* **2015**, *35*, 667. [Crossref]
63. Domingues, R. R.; Trugilho, P. F.; Silva, C. A.; A, I. C. N.; Melo, C. A.; Magriotis, Z. M.; Sa, M. A.; Melo, D.; *PLoS One* **2017**, *12*, 1. [Crossref]
64. Vassilev, S. V.; Baxter, D.; Andersen, L. K.; Vassileva, C. G.; *Fuel* **2010**, *89*, 913. [Crossref]
65. Tomczyk, A.; Sokołowska, Z.; Boguta, P.; *Fuel* **2020**, *278*, 118168. [Crossref]
66. Wu, W.; Yang, M.; Feng, Q.; Mcgrouther, K.; Wang, H.; Lu, H.; Chen, Y.; *Biomass Bioenergy* **2012**, *47*, 268. [Crossref]
67. Solantausta, Y.; Oasmaa, A.; Sipil, K.; Lindfors, C.; Lehto, J.; Autio, J.; Jokela, P.; Alin, J.; Heiskanen, J.; *Energy Fuels* **2012**, *26*, 233. [Crossref]
68. Lehto, J.; Oasmaa, A.; Solantausta, Y.; Kytö, M.; Chiaramonti, D.; *VTT Publications* **2013**, 79. [Crossref]
69. Oasmaa, A.; Solantausta, Y.; Arpiainen, V.; Kuoppala, E.; Sipilä, K.; *Energy Fuels* **2010**, *24*, 1380. [Crossref]
70. Auersvald, M.; Macek, T.; Schulzke, T.; Staš, M.; Šimáček, P.; *J. Anal. Appl. Pyrolysis* **2020**, *150*, 104838. [Crossref]
71. Song, Q.; Nie, J.; Ren, M.; Guo, Q.; *Energy Fuels* **2009**, *23*, 3307. [Crossref]
72. Oasmaa, A.; Elliott, D. C.; Korhonen, J.; *Energy Fuels* **2010**, *24*, 6548. [Crossref]
73. Wienhage, G. H.; Ramos, E. S.; Chiarello, L. M.; Botton, V.; Wiggers, V. R.; *Angolan Mineral, Oil Gas J.* **2021**, *2*, 21. [Crossref]

Submitted: December 30, 2025
Final version online: May 5, 2026